Extrapulmonary benign and malignant lesions avid for 18F-fluoro-deoxyglucose by multivariate regression model identification

CHEN Yangchun[1,2,*] XU Hao[1] CHEN Ping[2]

[1]*Department of Nuclear Medicine in the First Affiliated Hospital of Jinan University, Guangzhou 510632, China*

[2]*PET/CT Center in the First Affiliated Hospital of Guangzhou Medical College, Guangzhou 510230, China*

Abstract Whether extrapulmonary lesions are avid for ^{18}F-fluorodeoxyglucose (^{18}F-FDG) could help to differentiate the benign or malignant lung lesions. In this trial, the 199 consecutive patients with newly diagnosed lung lesions (169 malignant and 36 benign lesions) were imaged by whole body ^{18}F-FDG PET/CT. Histopathology and clinic results served as the reference standard. The malignancy likelihood were conducted by CT_{scores}; the maximum standardized uptake value (SUV_{max}) of lung lesions, and PET on FDG negative or positive, as well as metastasis index (*MI*), by PET combined with CT findings. The data were analyzed by stepwise logistic regression and receiver-operating-characteristic. The malignancy predictive probability (*P*) was obtained by $P = e^x/(1+e^x)$, where $x = -1.16+0.87\ (CT_{score}) +0.15(SUV_{max})+0.27(MI)$. The area under curve (AUC) for the fitted logistic model was 0.82±0.04, this was superior and significantly different from SUV_{max}(AUC, 0.73±0.05) and CT_{scores}(AUC, 0.71±0.05). The fitted logistic model could improve the diagnostic performance. The *MI* could help for differential diagnosis.

Key words Lung neoplasm, ^{18}F-fluorodeoxyglucose, Positron-emission tomography and computed tomography, Logistic models, Receiver-operating-characteristic

1 Introduction

As the differential diagnosis of pulmonary nodules and mass lesions in many countries, the positron emission tomography (PET) with ^{18}F-fluorodeoxyglucose (^{18}F-FDG) has been established. According to a meta-analysis of the published data on ^{18}F-FDG–PET scanning from January 1996 to September 2000, the average sensitivity and specificity of ^{18}F-FDG–PET scanning for detecting a malignancy was 97% and 78%[1]. The ^{18}F-FDG–PET has not the benefit of evaluating pulmonary nodules with low ^{18}F-FDG avid[2]. Compared with ^{18}F-FDG–PET, the combination of ^{18}F-FDG–PET with the diagnostic CT scan without intravenous contrast can improve the sensitivity from 69% to 97%, and does not change the specificity[3]. The diagnostic accuracy of ^{18}F-FDG PET/CT without the quality CT of lung nodule was similar with that of ^{18}F-FDG–PET[4,5]. Nie *et al.*[6] reported a semiautomatic computer-assisted diagnostic (CAD) scheme, indicating that the combination of ^{18}F-FDG–PET with CT can differentiate benign from malignant pulmonary nodules, and is better than ^{18}F-FDG–PET or CT alone. In that study, we excluded two nodules with extrathoracic malignancy, and focused on lung lesions in the whole body ^{18}F-FDG–PET. Lesion outside of lung cancer avid for ^{18}F-FDG is considered as metastasis. The extrapulmonary lesion is avid for ^{18}F-FDG, indicating that the newly diagnosed lung lesion is malignant.

2 Methods and materials

2.1 Patient cohort

With a lung lesion newly diagnosed at the conventional chest radiography or the X-ray CT for a suspicious malignant primary, the patients underwent whole body integrated ^{18}F-FDG PET/CT from February 2005 to January 2009. We selected the pathological confirmation and suspicious infection

Supported by National Natural Science Foundation of China [Grant No. 30800274]

* Corresponding author. *E-mail address*: fudanzhsh@yahoo.com.cn

Received date: 2012-10-20

patients cured by antibiotic, and excluded the patients with recent malignancy history and diabetes mellitus.

We gained the approval of Institutional Review Boards without patient informed consent.

The 199 consecutive patients (63 women and 136 men, 25–88 years old, mean age±*SD*: 58.8±12.4) met the further analysis criteria. In 205 lung lesion patients, their biopsy or surgery proved that the 169 was malignant; and 32, benign in pathology; and 4 infection cured by antibiotics (Table 1).

Table1 Frequency of lesions diagnoses (n=205)

Malignants	Numbers	Benigns	Numbers
Adenocarcinoma	101	Tuberculosis	11
Squamous cell carcinoma	34	Sarcoidosis	2
Adenosquamous carcinoma	4	Organized pneumonia	4
Large cell carcinoma	1	Abscess	4
Small cell carcinoma	10	Cryptococcal pneumonitis	1
Synoviosarcoma	1	Infection/inflammation	10
Hodgkin's lymphoma	1	Other benign lesions were not further classified	4
Metastatic carcinoma from rectum/ lung	3		
Unspecified NSCLC	14	/	/
Total number	169	/	36

2.2 Acquisition of PET/CT image

To fulfill the blood glucose level of less than the 8.3 mmol/dL, patients were asked to fast over 6 h and rest for 15 min before administration 5-MBq/kg ^{18}F-FDG. The images were acquired by a whole-body PET/CT scanner (Discovery DST 8; GE Healthcare, USA) after injection at 60 min. The whole body scan was approximately from the middle thighs to the skull roof. The CT scan without intravenous contrast was used as a protocol involving 140 kV, 150 mA, 0.8 s per tube-rotation, and 3.75-mm slice thickness. The PET scan was performed with a 3.27-mm section thickness, 3.5 min per table position, and two-dimensional acquisitions. Patients were asked to maintain normal shallow respiration during image acquisition.

The ^{18}F-FDG-PET images were reconstructed using CT attenuation correction and an ordered subset expectation maximization algorithm. The maximum standardized uptake value ($SUV_{\max}$) was determined by Ref.[7].

2.3 Acquisition of CT images

All patients underwent a breath-hold spiral CT scan on the lung lesions without intravenous contrast by 120kV, 170 mA, 0.8 second per tube-rotation, 2.5-mm slice thickness, and 1.35-pitch after PET/CT scan.

2.4 Interpretation of CT images

The CT images were interpreted by two radiologists, who were unaware of each patient's history and PET images. Each lesion was described by its site, size, attenuation, shape, margin characteristics, consolidation, cavitation, and invasion. The criteria for interpreting lesions were applied[5]. Readings in case of differing results were performed in consensus.

2.5 Interpretation of PET/CT images

The ^{18}F-FDG–PET criteria for malignancy were used as citation[8]. The locations of abnormal tracer uptake were recorded, and the metastasis index (*MI*) was scored by a 5-points scale (Table 2). The PET/CT images were analyzed by two doctors with experience of 5 years in the ^{18}F-FDG PET/CT. Also readings were conducted in consensus in case of differing results.

2.6 Statistical analysis

The patient characteristics were compared by the Student’s *t*-test and the chi-squared test. When the expected values in the any cells of the contingency table were below five, the Fisher exact test was conducted. Variables reaching the significance might be included in a multivariate logistic regression model. Selection method with entry testing was based on the significance of the score statistic; and removal testing, the probability (P>0.15) of the likelihood ratio test[9]. Odds ratios (*OR*) and the 95% CIs were computed by unconditional logistic regression. A receiver-operating -characteristic (ROC) analysis included the CT interpretations, and the lesion uptakes in $SUV_{\max}$, and

the predicted malignancy probability (P) which was calculated by the fitted multivariate logistic regression model. The difference in the area under curve (AUC) was tested by the Z statistic. A 2-tailed p values (≤ 0.05) showed statistical significant differences. The diagnostic OR for a test is defined as sensitivity/(1–sensitivity) ×specificity/(1–specificity)[10].

3 Results

3.1 Results of CT and PET/CT

The patient characteristics and their lesions are shown in Table 2. In the 58 lesions, their lesion sizes could hardly be determined because of the local atelectasis and its associated obstruction, and parahilar location. In the 147 lesions, the lesion sizes were 36±21 mm in the range of 4–143 mm). Locations of distant lesions avid for ^{18}F-FDG are listed in Table 3.

The non-contrast CT shows that 62% (104/169) of malignant lesions were classified as positive; and 29% (59/205) of all lesions, equivocal; and 44% (16/36) of benign lesions, negative (Table 2). Taking equivocal lesion as malignancy, the diagnostic OR was 8.2; and as benignancy, 3.6.

In Table 2, the sensitivity for ^{18}F-FDG PET/CT was 95% (161/169) and the specificity was 25% (9/36) at the diagnostic OR of 6.7. The sex, age, and lesion sizes were no obvious difference between benign and malignant lesions, but the CT_{score}, SUV_{max}, ^{18}F-FDG$_{\text{score}}$, and MI were highly different (p<0.01).

Table 2 Characteristics of patients and lesions

Characteristic		Malignancy	Benignancy	p
Patients	Women/Men	50/113	13/23	0.58
	Age / year	59±13	57±12	0.29
Lesions	Size (mm)[a]	37±22(n=122)	31±20 (n=25)	0.21
	CTscore (0/1/2)	15/50/104	16/9/11	<0.01
	18F-FDGscore(0/1)	8/161	9/27	<0.01
	SUVmax	10.7±6.0	5.7±3.7	<0.01
	MI(0/1/2/3/4)[b]	48/11/34/15/61	21/1/7/3/4	<0.01

[a] It was hard to measure the 58 lesions. [b] The lesions avid for ^{18}F-FDG in the lung hilar nodes was scored as 1; and ipsilateral mediastinal nodes, as 2; and contralateral mediastinal nodes, as 3; and distant locations, as 4. There was not any suspicious metastasis for the scored as 0.

Table 3 The location of distant lesion avid ^{18}F-FDG

Location/number	Malignancy	Benignancy
Celiac lymph nodes	8	2
Retroperitoneal lymph node	8	1
Pelvic lymph nodes	2	1
Inguinal lymph nodes	1	1
Lymph node of neck	12	/
Axillary nodes	4	/
Tonsil	1	/
Skeleton	26	1
Liver	5	1
Suprarenal gland	7	/
Brain	3	/
Cervical cord	1	/
Thyroid gland	/	1
Abdominal wall	1	/
Subcutaneous soft tissue	2	/
Gluteus	1	/
Pulmonary trunk and left atrium	1	/
Total number	83	7

3.2 Multivariate stepwise logistic regression model analysis

By stepwise selection, CT_{score}, SUV_{max}, and MI were included in the fitted multivariate logistic regression model without ^{18}F-FDG_{score}. In this model, when increasing, either CT_{scores} or SUV_{max} or MI was used as malignancy predictors. The P was calculated by $P=e^x/(1+e^x)$, where $x = -1.16+0.87(CT_{score})+0.15\ (SUV_{max}) + 0.27(MI)$ (Table 4).

Table 4 Variables in the fitted multivariate logistic models of 205 lung lesions (dependent variable malignancy/benignancy) by stepwise selection

Variables	Coefficient ($\beta \pm SD$)	Odds Ratio (95% confidence interval)	p
CT_{score} (0/1/2)	0.87±0.27	2.39(1.41–4.05)	<0.01
SUV_{max}	0.15±0.05	1.16(1.04–1.29)	<0.01
MI(0/1/2/3/4)	0.27±0.14	1.31(1.00–1.73)	0.05
Constant	–1.16±0.47	0.31(0.12–0.79)	0.01

The model estimated that the P was more than 50% at $x \geq 0$. The CT_{score} calculated by the equation was 2 at $x>0$. In other words, at the positive CT scan, the lung lesion should be taken as malignancy regardless of ^{18}F-FDG uptake[3]. For example, an adenocarcinoma in the right upper lobe was noted, its CT_{score} was 2; and SUV_{max}, 1.5; and MI, 0; and P, 69.1%, as shown in Fig.1.

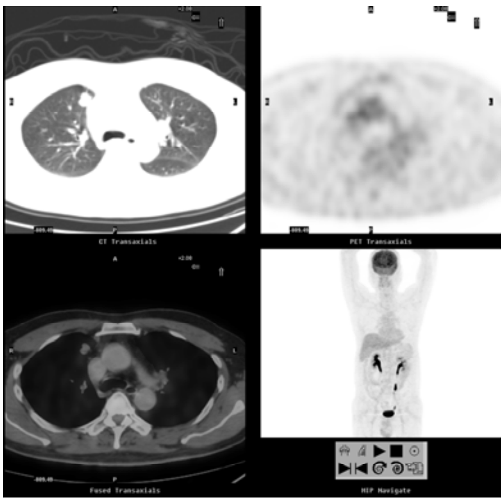

Fig.1 The ^{18}F-FDG-PET/CT images of an adenocarcinoma.

At the same time, when CT_{score} was 1 and SUV_{max} was not less than 2, the x was larger than zero. To put it at the indeterminate CT scan, the SUV_{max} =2.0 was used as cutoff for malignancy[3,11], thus helping to distinguish between benign and malignant lesions. When CT score was zero, the x was larger than zero at the SUV_{max} of larger than 7.7, suggesting that the lung lesion should be considered as malignancy regardless of its morphological information. When diagnostic results of CT_{score} were contradictive with the SUV_{max}, the MI could help for differential diagnosis. For example, an inflammation lesion in the left lower lobe was observed, its CT_{score} was zero; and SUV_{max}, 5.0; and MI, zero; and P, 39.9% (Fig.2).

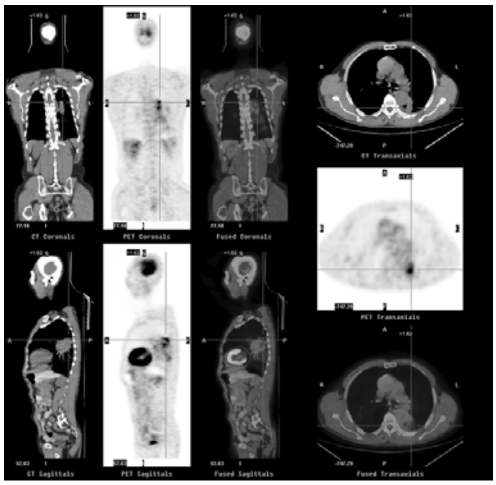

Fig.2 The ^{18}F-FDG-PET/CT images of an inflammation lesion.

3.3 ROC analysis

A ROC analysis for CT_{score}, SUV_{max} and P was performed (Fig.3). The SUV_{max} curve based on the lung lesions has the cutoff of initial 1.5, step 0.5, and end 8.0. The SUV_{max} curve intersects the CT_{score} curve. The additional values on CT_{score} and SUV_{max} curves hold over the entire range of sensitivity and specificity. The AUC was 0.83±0.04 for the model; and 0.71±0.05, for CT_{score}; and 0.74±0.05, for SUV_{max}. Statistical analysis by the AUC shows that the model was superior and significantly different from SUV_{max} (p=0.01) and CT_{score} (p<0.01). There was no significant difference between SUV_{max} and CT_{score} at p=0.64. At the cutoff value of 0.50 for malignancy, the

sensitivity was 96% (163/169); and specificity, 31% (11/36); and the diagnostic *OR* for *P*, 12.0.

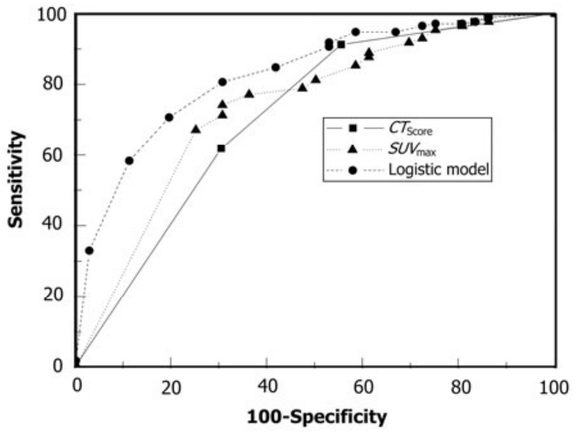

Fig.3 A receiver-operating -characteristic (ROC) analysis.

4 Discussion

In the ^{18}F-FDG–PET, the SUV_{max} at OR=1.16 (p<0.01) was associated with lung malignancy in the model (Table 4). The SUV_{max} increased as a significant malignancy predictor was similar to Grgic's report [10]. The sensitivity of ^{18}F-FDG PET/CT scanning for detecting malignancy was 95%, this was equivalent to the available data of 97% sensitivity by meta-analysis[1], and a prospective multicenter study of 92% sensitivity[8]. But the 25% specificity in our study was lower than those of the reported 44%–85%[1,3-5,8,11-13]. Also, the benign lesions, including tuberculosis, bacterial pneumonia, organized pneumonia, active sarcoidosis, infectious granulomas, and acute pyogenic abscesses, and so forth, can produce false-positive readings in ^{18}F-FDG–PET[14], these were mainly caused by the low specificity.

The CT morphological information was an effective predictor for malignancy at OR=2.41(p<0.01), and its sensitivity and specificity were not as accurate in this study as in a multicenter of contrast-enhanced CT (98% sensitivity, and 58% specificity)[15]. As we know, a lung lesion at CT diagnosis suspicious for a malignant primary is usually dependent on morphological information and enhancement[16]. Some equivocal lesions may shift to definitely malignant or definitely benign on its enhancement, and improve the CT sensitivity and specificity. The less accuracy was likely caused without contrast-enhanced CT[15].

The *MI* was included in the model at OR=1.31(p=0.05). To the best of our knowledge, the *MI* is the first proof whether lesions outside of lungs avid for ^{18}F-FDG might help to distinguish the malignant lung lesion. Based on the score statistic probability (p=0.05), we should be cautious to make a conclusion by *MI*.

The ^{18}F-FDG_{score} was excluded from the model because its information had been included in its SUV_{max}. The stepwise logistic regression was designed to find the most parsimonious set of predictors in predicting malignancy.

The ROCs show that the model lies over the curve for CT diagnosis and SUV_{max}, indicating that the model accuracy is superior regardless of where setting the threshold defining a malignancy test. Furthermore, the statistical test by the AUC shows that the superior model was different from CT_{score} and SUV_{max}. Compared with the diagnostic *OR* of 3.7 or 8.3 in different diagnosis protocol for CT and ^{18}F-FDG (6.3), the diagnostic *OR* reached the highest value of 12.0 at the cutoff of 0.50 *P*, suggesting the model was better than CT and SUV_{max} alone. The model had potential to develop a semiautomatic CAD to aid and improve physician diagnostic skills, and it would be tested by a multicenter in the future.

5 Limitation

In this retrospective clinical study, our patients were selected from their larger pool, and referred to the ^{18}F-FDG PET/CT study because of the pathologic verification of their lung lesions, these induced a selection bias. The malignancy rate was 82% (169/205). No matter how there were several influencing factors such as serum glucose level, respiration, partial-volume effects, and noises[17], the SUV_{max} was in use as the de facto standard[18].

6 Conclusion

In this study, the extrapulmonary lesions avid ^{18}F-FDG could distinguish the malignancy from benignancy. Our logistic model including CT_{score}, SUV_{max}, and *MI* information for predicting the malignancy *P* was superior to CT and ^{18}F-FDG alone, thus improving physician diagnostic performance.

Acknowledgments

We thank Dr Xin Cai in the PET center of the First Affiliated Hospital of Guangzhou Medical College in China who had contributed to get CT images interpretation to us.

References

1 Gould M K, Maclean C C, Kuschner WG, *et al.* JAMA, 2001, **285:** 914–924.

2 Kim S K, Allen-Auerbach M, Goldin J, *et al.* J Nucl Med, 2007, **48:** 214–220.

3 Chen Y C H, Chen, P, Tian J H, *et al.* Nucl Sci Tech, 2009, **20:** 17–21.

4 Pauls S, Buck A K, Halter G, *et al.* Mol Imaging Biol, 2008, **10:** 121–128.

5 Nie Y, Li Q, Li F, *et al.* J Nucl Med, 2006, **47:** 1075–1080.

6 Boellaard R, O'Doherty M.J, Weber W.A, *et al.* Eur J Nucl Med Mol Imaging, 2010, **37:** 181–200.

7 Fletcher J W, Kymes S M, Gould M, *et al.* J Nucl Med, 2008, **49:** 179–185.

8 Hosmer D W, Lemeshow S. Applied logistic regression. 2nd edition. New Jersey: John Wiley & Sons, Inc, 2000, 31–142.

9 Eadie, L.H, Taylor P, Gibson A. Eur J Radiol, 2012, **81:** e70–e76.

10 Grgic A, Yüksell Y, Gröschel A, *et al.* Eur J Nucl Med Mol Imaging, 2010, **37:** 1087–1094.

11 Suga K, Kawakami Y, Hiyama A, *et al.* Ann Nucl Med, 2009, **23:** 427–435.

12 Tian J H, Yang X F, Yu LJ, *et al.* J Nucl Med, 2008, **49:** 186–194.

13 The American College of Radiology. Acr practice guideline for performing FDG-PET/CT in oncology. ACR. 2007. http:// www.acr.org/ Secondary MainMenu Categories/ quality_safety /guidelines/ nuc_med/ fdg_ pet_ct.aspx (June 18, 2009).

14 Swensen S J, Viggiano RW, Midthun D E, *et al.* Radiology, 2000, **214:** 73–80.

15 Lee K.S, Yi C A, Jeong S Y, *et al.* Chest, 2007, **131:** 1516–1525.

16 Basu S, Zaidi H, Holm S, *et al.* Curr Med Imaging Rev, 2011, **7:** 216–233.

17 Wahl R L, Jacene H, Kasamon Y, *et al.* J Nucl Med, 2009, **50:** 122S–150S.